Electronic Supplementary Material (ESI) for Journal of Materials Chemistry C.

A Fluorescent Dithiadiazolyl Radical: Structure and Optical Properties of Phenanthrenyl Dithiadiazolyl in Solution and Polymer Composites

Yassine Beldjoudi, Igor Osorio-Roman, Mitchell Nascimento and Jeremy M. Rawson*

Electronic Supplementary Information

ESI-1 Single Crystal X-ray diffraction.

Brown plate-like crystals of **2** were mounted on a cryoloop using paratone oil and data were collected using ϕ and ω scans at 173(2) K on a Bruker D8 Venture four circle diffractometer equipped with a Photon CCD detector using Mo-Kα radiation. Data were integrated using APEX-II [Bruker AXS, Madison, WI, USA] and an absorption correction applied using SADABS [Bruker AXS, Madison, WI, USA]. The structure was solved by direct methods to reveal one dimer (two molecules) in the asymmetric unit. All non-H atoms were refined anisotropically and H-atoms were added at calculated positions and refined with a riding model. Structure solution and refinement was undertaken within the SHELXTL suite [Bruker AXS, Madison, WI, USA]. A summary of crystallographic data is presented in Table S.1. Both structures are available free of charge from the Cambridge Crystallographic Data Centre (CSD deposition number: 1443722).

Table S.1: Crystallographic data for pristine **2**

Parameters	**2**
Formula	$C_{15}H_9N_2S_2$
FW	281.36
Temp. (K)	173(2)
Crystal system	Monoclinic
Space group	$P2_1/c$
a/Å	7.5618(9)
b/Å	9.5721(11)
c/Å	32.633(4)
α/°	90.00
β/°	92.446(3)°
γ/°	90.00
V/Å^3	2359.9(5)
Z	8
D_c/Mg m^{-3}	1.584
μ(MoKα)/ mm^{-1}	0.43
Unique reflns	4777
Reflns [I>2σ(I)]	3776
R_{int}	0.046
R_1 (I> 2σ(I)), wR_2 (all)	0.061, 0.139

ESI-2 Cyclic Voltammetry

Cyclic voltammograms were measured on a CH Instruments electrochemical work station model CHI760E. A solution was prepared in CH_2Cl_2 comprising 0.05 M 2 and 0.10 M supporting electrolyte, $[Bu_4N][PF_6]$ and examined within a honeycomb spectro-electrochemical cell (Pine Research Inst.) using an Ag/AgCl reference electrode. Measurements were performed with a scan rate of 0.05 V/s and the ohmic capacitance of the solution was automatically compensated. A reversible redox process was observed at $E_{1/2}$ = +0.68 V.

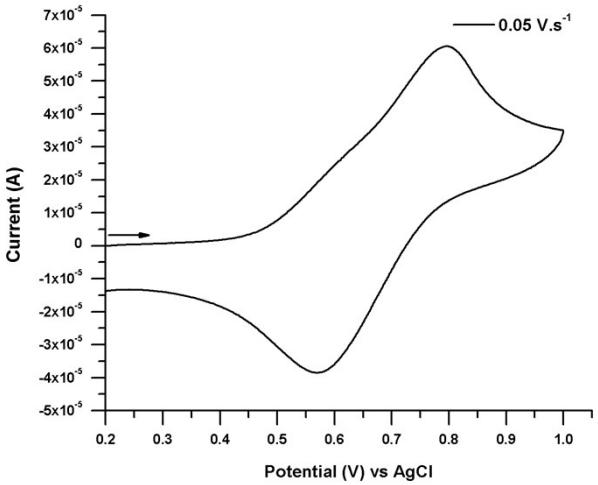

Figure S.1 Cyclic voltammogram of **2** in CH_2Cl_2

ESI-3 Absorption and Fluorescence studies

All UV-visible spectroscopic studies were conducted on a G103A Agilent spectrophotometer. Fluorescence spectroscopy was carried out on a Varian fluorescence spectrometer.

ESI 3-1 In Solution

Absorption and emission spectra of phenanthrene carbonitrile (**3**), **2** and [**2**][$GaCl_4$] in MeCN are shown below (Fig. S2). The absorption and emission profiles of **2** and [**2**][$GaCl_4$] are essentially identical. The absorption spectrum of **2** shows little solvent dependence whereas emission spectra show a marked solvatochromic shift in λ_{max} (Fig. S3). Data are summarised in Table S.2.

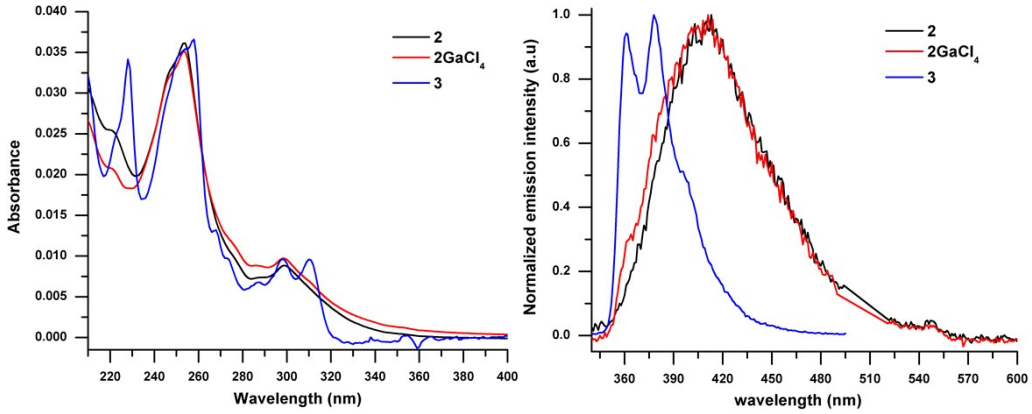

Figure. S2 Left: absorption profile of phenanthrene derivatives in MeCN ($4x10^{-7}$ M) (**3** = phenanthrene carbonitrile). Right: Emission spectra of phenanthrene derivatives in MeCN ($4x10^{-7}$ M) under 256 nm excitation.

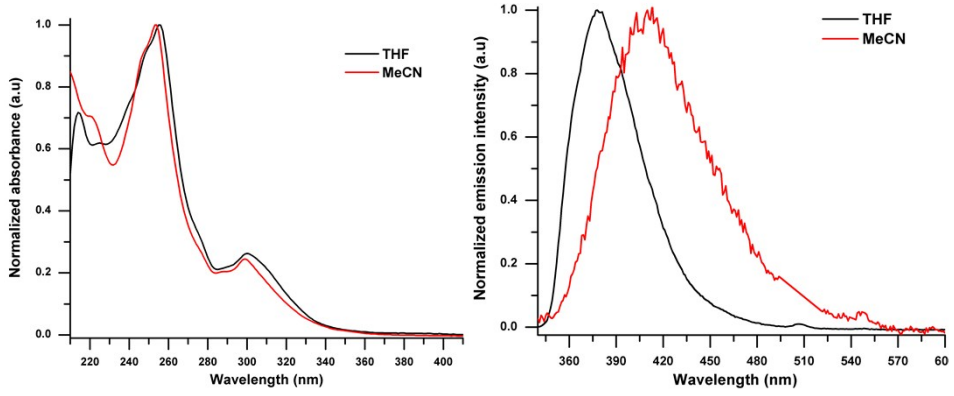

Figure. S3 Solvatochromic effect on the absorption (left) and emission (right) profiles of **2** in MeCN and THF solution (4×10^{-7}M) [excitation wavelength: 256 nm].

Table S.2 UV-visible and fluorescence parameters of **2**, [**2**][$GaCl_4$] and **3** (phenanthrene carbonitrile)

Compound	*C* (mol.l^{-1})	λ_{max} (nm)	Absorbance (a.u)	ε (M.cm^{-1})	λ_{exc} (nm)	λ_{em} (nm)	Φ_F*
2	4×10^{-7}	254	0.0412	103000	254	410	0.1138
		298	0.0139	34750	298	410	0.0956
[**2**][$GaCl_4$]		254	0.0405	101250	254	410	0.3454
		298	0.0121	30250	298	410	0.3571
PhenCN (**3**)		258	0.0368	92000	258	378	0.5035
		298	0.0104	26000	298	378	0.677

*Diphenyl anthracene (DPA) was used as a standard (Φ_F = 0.88 in ethanol)[1]

ESI-3-2 Thin Film Studies in Polystyrene

Thin films of **2** in PMMA and PS were prepared by drop-casting with *w/w* ratios from 1:75 to 1:1000 to examine the effect of concentration (aggregation). Thin films of **2**:PS show the expected increase in absorption with increasing *w/w* content of radical (Figure S.4). Conversely the emission profile showed a strong emission at high dilution (1:1000) at 360 nm which was quenched with increasing radical concentration consistent with aggregation-induced-quenching.

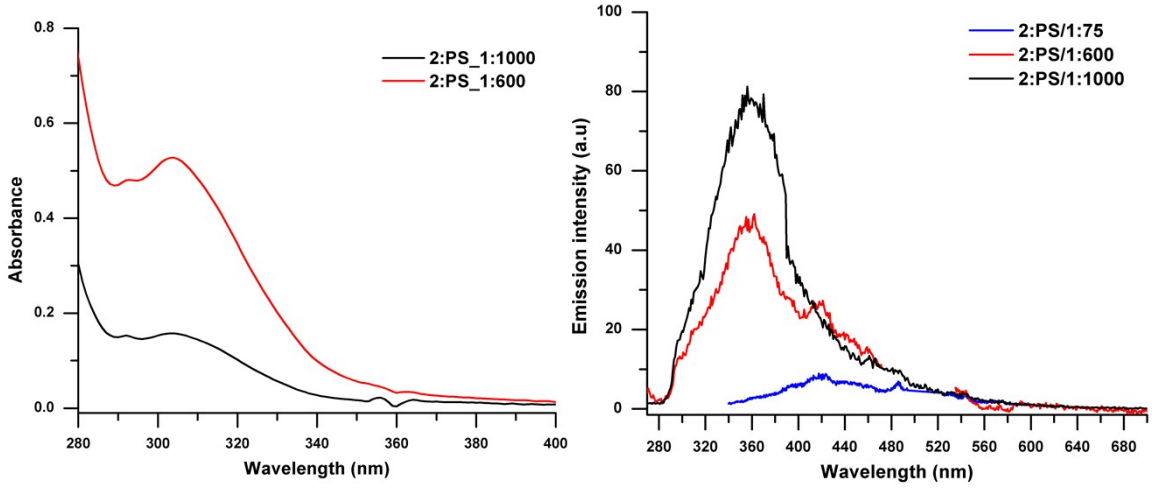

Figure S.4 Left: absorption spectra of **2**:PS composite films at different *w/w* ratios. Right: emission spectra of **2**:PS composite films at different *w/w* ratios [Excitation wavelength: 256 nm].

ESI-4 TD-DFT Calculations

The structure of **2** was geometry optimised at the UB3LYP/6-311G*+ level and time-dependent DFT calculations were carried out on the optimised gas-phase geometry using Jaguar[2] considering a total of 100 excited states to reach to the upper end of the absorption spectrum (200 nm). Good agreement was achieved between the positions of the calculated and experimental profiles (Fig. S.5). Twelve transitions were determined with oscillator strengths > 0.1 and these are tabulated in Table S.3. The one-electron frontier orbitals (α and β spins) relevant to the transition at 253 nm are presented in Fig. S.6. This transition is not associated with a single dominant configuration amongst the excitation amplitudes and the major contributions to this transition are given in Table S.4. It is noteworthy that none of these involve the radical electron (α-73).

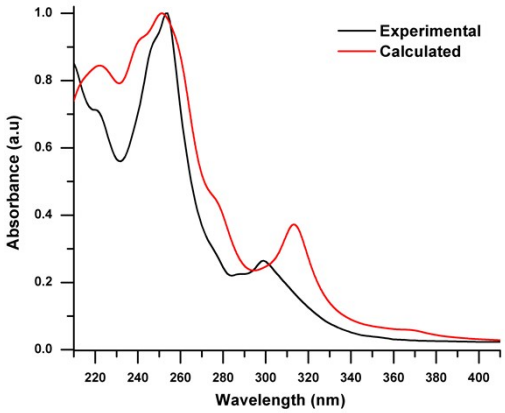

Figure S.5 Experimental (black) and calculated (red) UV/visible spectra for **2**.

Table S.3 UB3LYP/6-311G*+ computed transitions for **2** with oscillator strengths (*f*) greater than 0.1

Transition	Wavelength(nm)	*f*	transition dipole moment (Debye)
21	313.6	0.375	5.00
27	277.9	0.245	3.81
34	260.9	0.412	4.78
39	253.5	0.226	3.49
40	250.5	0.406	4.65
46	240.5	0.177	3.01
48	239.4	0.338	4.15
57	227.6	0.206	3.15
63	221.6	0.178	2.89
68	215.4	0.104	2.18
80	210.1	0.227	3.19
87	204.6	0.102	2.10

Table S.4 Contributions to the 253 nm excitation.

excitation	X coeff.	excitation	X coeff.
α(68) → α(75)	0.11079	β(69) → β(75)	–0.18918
α(69) → α(75)	–0.17713	β(70) → β(75)	0.44936
α(70) → α(76)	0.39193	β(70) → β(76)	–0.35877
α(71) → α(76)	0.24191	β(70) → β(78)	–0.12305
α(72) → α(75)	0.10989	β(71) → β(76)	0.20200
		β(71) → β(78)	–0.17406
		β(72) → β(78)	–0.34905
		β(72) → β(73)	0.14773

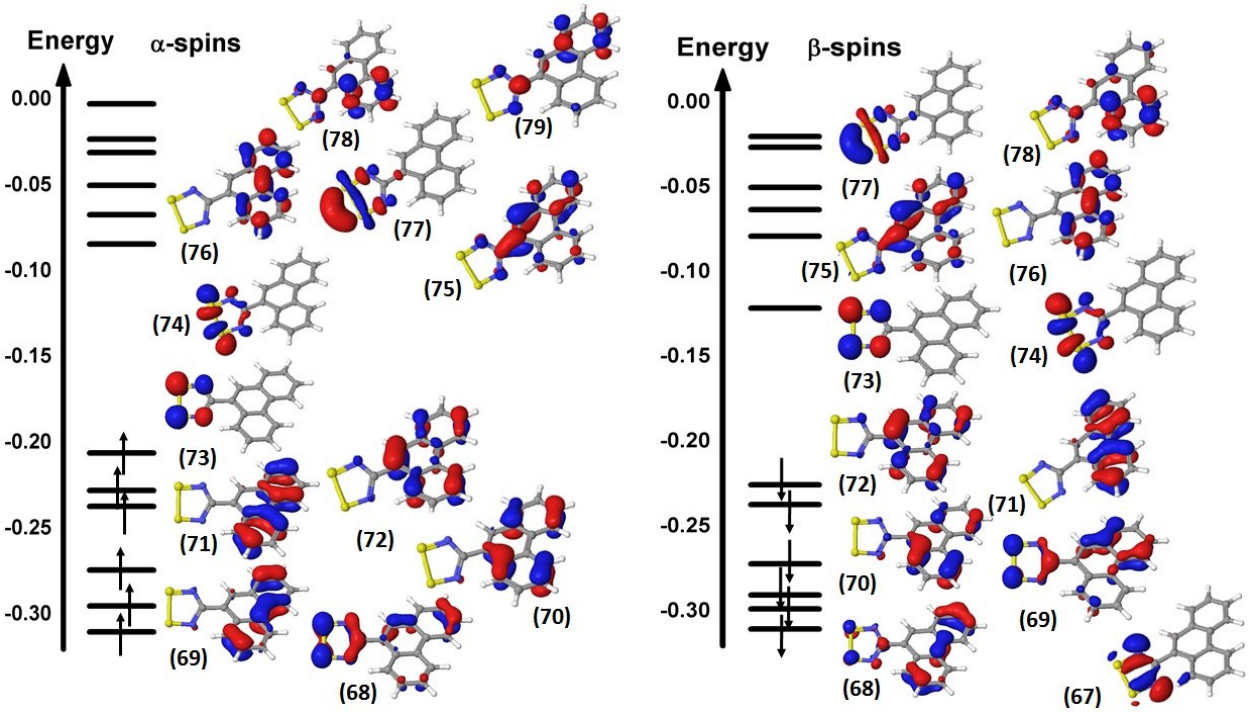

Figure S.6 One-electron frontier orbitals of the 'spin-up' α electrons and 'spin-down' β electrons based on UB3LYP/6-311G*+ calculations.

ESI-5 EPR spectroscopy

EPR spectra were recorded on a Bruker EMXplus X-band EPR spectrometer at room temperature.

5-1 Solution EPR spectroscopy

Radical **2** was dissolved in dry dichloromethane under nitrogen atmosphere. After the first measurement, the sample was exposed to air and the decay of the spectral intensity monitored by EPR spectroscopy (Fig. S.7). The kinetic of the decomposition of **2** followed a first order kinetics (Fig. S.7). A ln(I) *vs* t plot afforded k = 0.096 min^{-1} from which $t_{1/2}$ = 7.24 min.

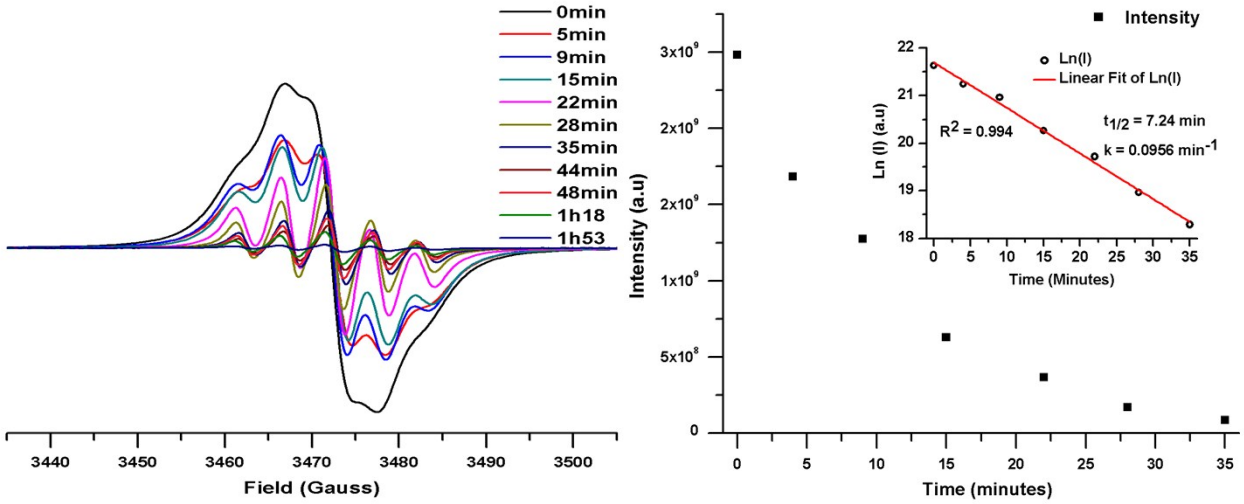

Figure S.7 (left) Time-dependence of the EPR spectra of **2** dissolved in CH_2Cl_2 exposed to air; (right) Plot of the EPR spectral intensity as function of time. Inset: Plot of ln(Intensity) *vs* time (R^2=0.99).

5-2 EPR Studies on 2:PMMA

A **2:PMMA** composite film (*w/w* ratio 1:75) was inserted within an EPR tube under nitrogen atmosphere. After the first measurement, the sample was exposed to air and the decay of the spectra intensity monitored by EPR spectroscopy (Fig. S.8). The kinetics of the decomposition of **2** followed second order kinetics over the first 6 hours (Fig. S.8). The time taken for the spectral intensity to drop to half its original value was 79 min.

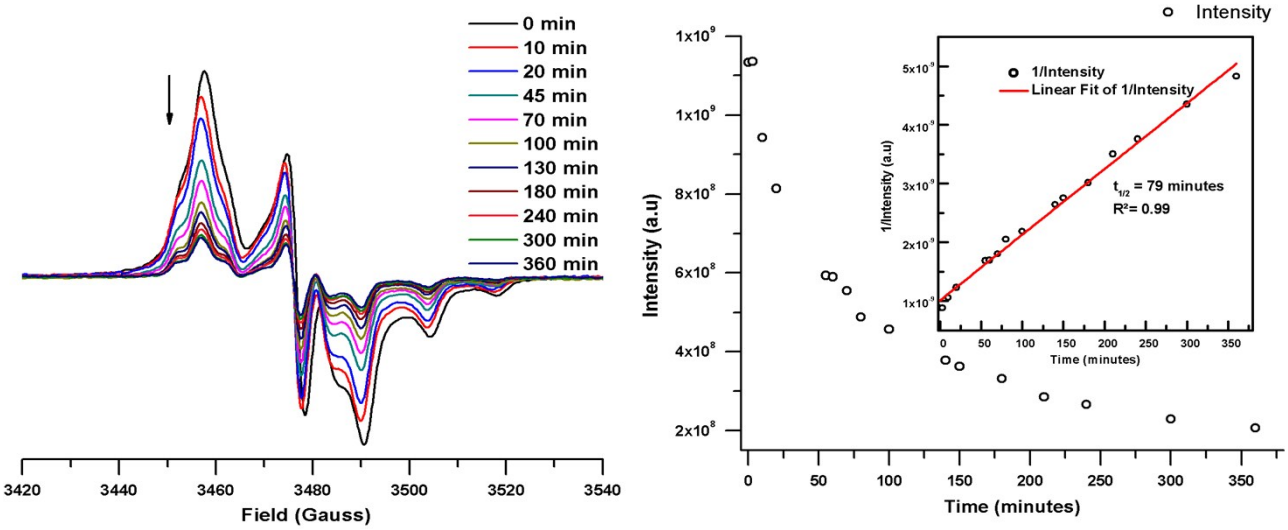

Figure S.8 (left) Time-dependence of the EPR spectra of **2**:PMMA (*w/w* ratio = 1:75) upon air exposure; (right) Plot of the intensity of the EPR spectra as function of time. Inset: Plot of 1/Intensity *vs* t indicating approximate second order kinetics (R^2 = 0.99).

5-3 EPR spectroscopy on 2:PS

A **2**:PS composite film (*w/w* ratio = 1:75) was inserted within an EPR tube under nitrogen atmosphere. After the first measurement, the sample was exposed to air and the decay of the spectral intensity monitored by EPR spectroscopy (Fig. S.9). The kinetics of the decomposition of **2**:PS did not show either first or second order kinetics. A general expression for isothermal reactions (Sharp-Hancock model) for solid state reactions was used to fit the data (Fig. S.9).[3]

$ln(-ln(1-\alpha))= m.ln(k) + m.ln(t)$

Where α is the normalized intensity [I_t/I_0] of the EPR signal, *k* is the rate constant and *m* depends upon the mechanism and *t* is the time. The EPR spectroscopy reveal a significant increase of the stability of **2** and the time taken for the sample intensity to decay to half its original intensity was estimated to be 1680 minutes.

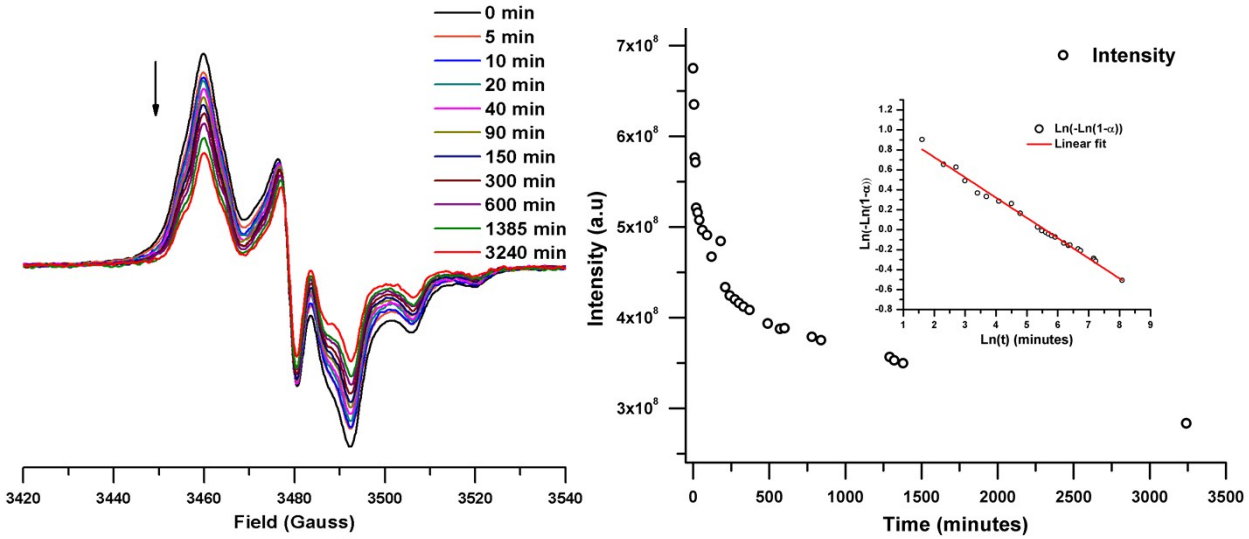

Figure S.9 (left) Time-dependence of the EPR spectra of **2**:PS (*w/w* ratio = 1:75) upon air exposure; (right) Plot of the intensity of the EPR spectra as function of time. Inset: A 'ln-ln' plot revealing a linear dependence (R^2=0.99).

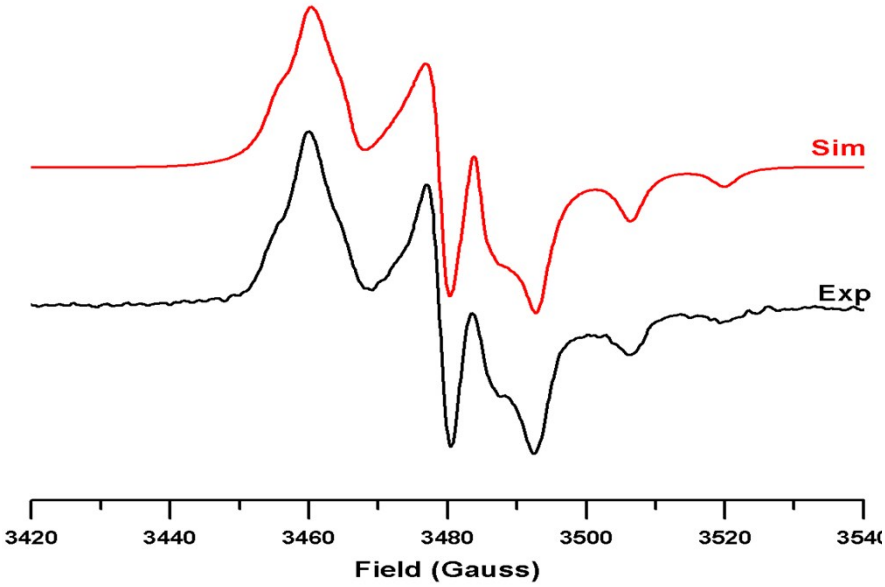

Figure S.10 Experimental and simulated spectra of **2**:PS. Simulation parameters: g_x =2.0205, g_y=2.0069, g_z=2.0021, a_x = 0.5, a_y= 2, a_z=13.5 G, ΔH_x= 2.5 G, ΔH_x= 1.7 G, ΔH_x=2.3 G [correlation=0.992].

References

1. E. A. Chandross, F. I. Sonntag, *J. Am. Chem. Soc.*, 1966, **88**, 1089-1096.
2. Jaguar v.8.7, Schrodinger, Inc., New York, NY, 2015; A. D. Bochevarov, E. Harder, T. F. Hughes, J. R. Greenwood, D. A. Braden, D. M. Philipp, D. Rinaldo, M. D. Halls, J. Zhang, R. A. Friesner, Jaguar: A High-Performance Quantum Chemistry Software Program with Strengths in Life and Materials Sciences, *Int. J. Quantum Chem.*, 2013, ***113***, 2110-2142.
3. H. Schmalzried, *Chemical kinetics of solids*, Wiley-VCH, Weinheim, Germany, 1995.